Evidence for deep mantle circulation from global tomography

R. D. van der Hilst*, S. Widiyantoro† & E. R. Engdahl‡

* *Massachusetts Institute of Technology, Department of Earth, Atmospheric, and Planetary Sciences, Rm 54-514, Cambridge Massachusetts 02139, USA*
† *Australian National University, Research School of Earth Sciences, Canberra ACT 0200, Australia*
‡ *US Geological Survey, DFC, MS 967, PO Box 25046, Denver, Colorado 80225, USA*

Seismic tomography based on P-wave travel times and improved earthquake locations provides further evidence for mantle-wide convective flow. The use of body waves makes it possible to resolve long, narrow structures in the lower mantle some of which can be followed to sites of present-day plate convergence at the Earth's surface. The transition from subduction-related linear structures in the mid-mantle to long-wavelength heterogeneity near the core–mantle boundary remains enigmatic, but at least some slab segments seem to sink to the bottom of the mantle.

Global tomography, a technique pioneered in the 1970s and early 1980s[1,2] to interpret the observed seismic wave field in terms of seismic properties at depth, is revolutionizing our knowledge of the Earth's interior. However, decades of research and spirited debate have not led to a consensus on the scale of mantle convection and the nature of coupling between motions in the deep interior and tectonic processes at the surface. Resolution of this issue is important for better understanding of the thermal and chemical evolution of our planet[3,4]. There is increasing agreement on large-scale (>4,000 km) structural features in global images[5–7], which represent the integrated effects of mantle processes over long periods of time[8,9]. The shorter-wavelength components in the models, however, have appeared sensitive to the type of data and model parametrization used in the inversions and have so far not shown convincing correlation. This lack of agreement prevents the effective use of global models to constrain reconstructions of past plate motion and numerical flow simulations at high Rayleigh numbers, and to discriminate unambiguously between end-member circulation models known as layered-mantle and whole mantle convection. For recent reviews see refs 6, 10–13.

Several lines of geophysical evidence support flow across the boundary between the upper and lower mantle, defined here by the seismic discontinuity at approximately 660 km depth. The magnitude of lateral variations in depth to this interface[14] is consistent with an endothermic phase change in the (Mg, Fe)$_2$SiO$_4$ system[15] that is by itself too weak to stratify flow[16]. Global tomography models lack the increased heterogeneity near 660 km depth expected for a thermal boundary layer at that depth[17], anomalous travel times of high-frequency waves are consistent with slab penetration into the lower mantle in some subduction systems[11,18–25], and long-wavelength gravity data can be explained by dynamic models of deep circulation in a high-viscosity lower mantle[5,12,26]. On the other hand, regional seismological studies have demonstrated stagnation of some slabs in the upper-mantle transition zone[20,21]. In addition, the long-term survival of distinct chemical reservoirs of primordial mantle as deduced from isotope and trace-element data has been used as evidence for layered convection (for reviews see refs 3 and 4). However, these data are not inconsistent with mantle-wide distribution of compositional heterogeneity[12,27], for which there seems to be increasing observational seismological evidence[28,29].

Here we present results of the inversion of carefully processed travel times, mainly from first-arriving P-waves, for aspherical variations in compressional wave speed in the Earth's mantle. The uneven sampling limits the resolution of aspherical structure in the upper mantle, but the new data reveal deep structure in unprecedented detail, which helps to assess the ultimate fate of the subducted slabs and their role in lower-mantle flow. We infer long, linear structures that locally connect to seismogenic slabs in the upper mantle and that divide the mid-mantle into large domains of shorter-wavelength heterogeneity. The transition from the linear subduction-related structures in the mid-mantle to long-wavelength heterogeneity near the core–mantle boundary (CMB) remains enigmatic, but our study reveals segments of slab that connect to structural heterogeneity in the CMB region. Along with results of regional studies that reveal structural complexity in the transition zone, these findings suggest that the Earth's present-day convective regime is predominated by some form of whole mantle overturn and their intermittent mantle stratification is a local[30] and transient[31,32] phenomenon only.

Data and tomographic method

Shear-wave models are often based on carefully processed digital waveforms and can exploit the excellent spatial data coverage provided by a combination of direct and surface-reflected body[22] and surface waves[33–35] and by constraints of free oscillation data[7,36]. In contrast, global P-wave models are typically based on relatively noisy short-period travel-time data reported to international data centres by thousands of station operators worldwide[1,2,5,21,37,38]. An important novel aspect of our global imaging is the use of better travel-time data and earthquake locations than previously available.

In a major effort, Engdahl and co-workers[39] reprocessed the entire database published by the International Seismological Centre (ISC) and, for recent years, the US Geological Survey's National Earthquake Information Center. Using robust statistics, an improved global travel-time model[40], and the arrival times of direct P- and S-phases, depth phases (pP, sP and the ocean-surface-reflected pwP), and PKP core phases, they relocated in an iterative, nonlinear procedure all teleseismically well-constrained earthquakes occurring between 1 January 1964 and 31 December 1995 (Fig. 1a). Upon application of appropriate corrections and event selection criteria, this procedure minimizes focal depth errors and the mapping of source heterogeneity into mislocation, thereby creating a significantly improved database for tomographic imaging. We used an iterative, conjugate-gradient algorithm[41] to invert all available P and pP travel-time residuals for effects of source mislocation due to three-dimensional structure and for P-wave speed in about 300,000 constant velocity blocks. We did not account for effects of aspherical structure on path geometry. This may underestimate the amplitude and overestimate the width of the anomalies in the upper mantle but does not effect the conclusions based on relatively large-scale lower-mantle structures.

The Earth's mantle is probably heterogeneous at all scales but the choice of a particular parametrization sets a minimum resolution length and excludes smaller structure from observation. Models based on spherical harmonics[33–36] constrain long-wavelength anomalies, but do not resolve in detail trajectories of mantle flow such as descending slabs. The local basis functions used in our study (constant-velocity blocks with a dimension of 2° × 2° × 200 km in the lower mantle) begin to provide the resolution required to investigate the continuity of structure between upper and lower mantle and the pattern of convective flow at larger depth. However, the uneven source/receiver distribution (Fig. 1a) and the effective restriction of inversions for P-wave speed to body waves necessarily renders large regions where the solution is not constrained, in particular in the upper mantle and transition zone (Fig. 1b). Body-wave sampling improves significantly in the mid-mantle (Fig. 1c–e) but degrades again in the lowermost mantle, especially in the Southern Hemisphere (Fig. 1f). Here we focus on the part of the solution pertinent to lower-mantle structure; detailed images of slabs in the upper mantle are better obtained by regional studies or global studies that allow for variable block size, which would ideally be based on three-dimensional ray tracing to account for effects of ray bending.

Aspherical mantle structure

Our results for the upper mantle (not shown) are in general agreement with surface-wave studies[6,7,33–35]; low wave speeds characterize marginal basins and tectonic continental regions, and zones of fast wave propagation outline stable continental cratons. The data reveal numerous fast anomalies in the upper-mantle transition zone beneath the circumpacific region (Fig. 1b), which agrees with inferences from Earth's free oscillations[36].

In the top half of the lower mantle, inversion of our improved data brings out prominent high-wave speed structures that continue intermittently over horizontal distances in excess of 10,000 km beneath the Americas and the southern margin of Eurasia (Fig. 1c, d). These outstanding structures correlate with anomalies in models based on spectral techniques (Fig. 2) but are narrower than inferred from these previous results, in particular at depths less than 1,500 km. With a width of 500–1,000 km in map view their shape is not controlled by the block size used. We infer that the

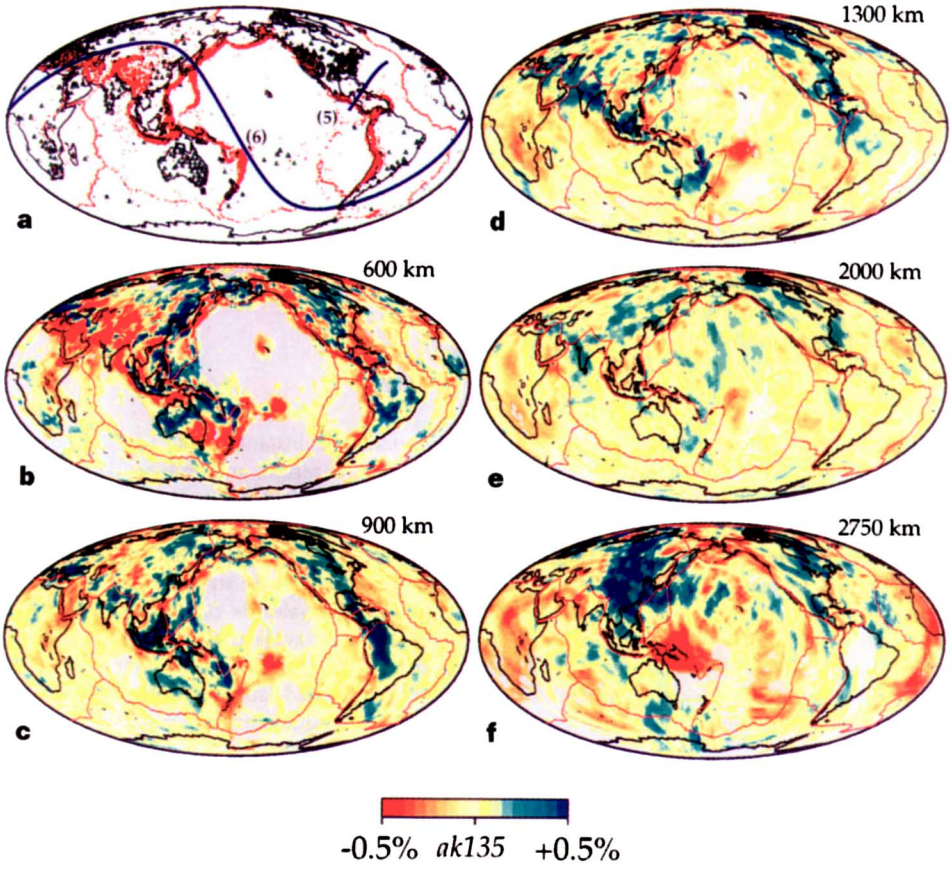

Figure 1 **a**, Pacific-centred Mollweide projection depicting the locations of the almost 80,000 earthquakes (red dots) and 3,500 stations (triangles) that produced the 7.3 million P and 0.3 million pP phases used in the inversions resulting in the P-wave-speed anomalies as displayed at 600 km (**b**), 900 km (**c**), 1,300 km (**d**), 2,000 km (**e**) and 2,700 km (**f**) depth in the Earth's mantle. Dark blue lines in **a** depict the locations of the cross-sections of Figs 5 and 6. To suppress noise and reduce the spatial imbalance in data coverage we grouped data associated with event and station clusters into summary rays[25], which reduced the total number of data used in the inversions from 7.6 million to 500,000. Wave speed variations are relative to the radially stratified *ak135* model[40]; see colour scale. Blue (red) colours represent fast (slow) wave propagation; grey depicts mantle regions of poor sampling. In these map views, no *a posteriori* smoothing or interpolation is used other than regridding from 2° × 2° to 1° × 1° blocks. The amplitude is, however, poorly constrained and therefore not used in the discussions. The perturbations may underestimate the actual values because of (1) the effect of regularization (damping) of the inversion, (2) trade-offs with earthquake location (on inversion, the hypocentre relocation parameters can in principle absorb substantial signal; in practice this is limited by the effective control on focal depth by the depth phases[39]), and (3) the neglect of ray bending effects. The regularization applied is a combination of norm and gradient damping; in absence of strong data constraints the former produces a bias towards the reference values (that is, zero anomalies) and the latter minimizes the difference in amplitude between adjacent blocks, which results in a smooth model. The model shown reduces the variance of the summary ray data by almost 50%, in addition to the ~15% variance reduction pre-processing of the original ISC data[20,39]. The thin red lines depict the location of plate boundaries.

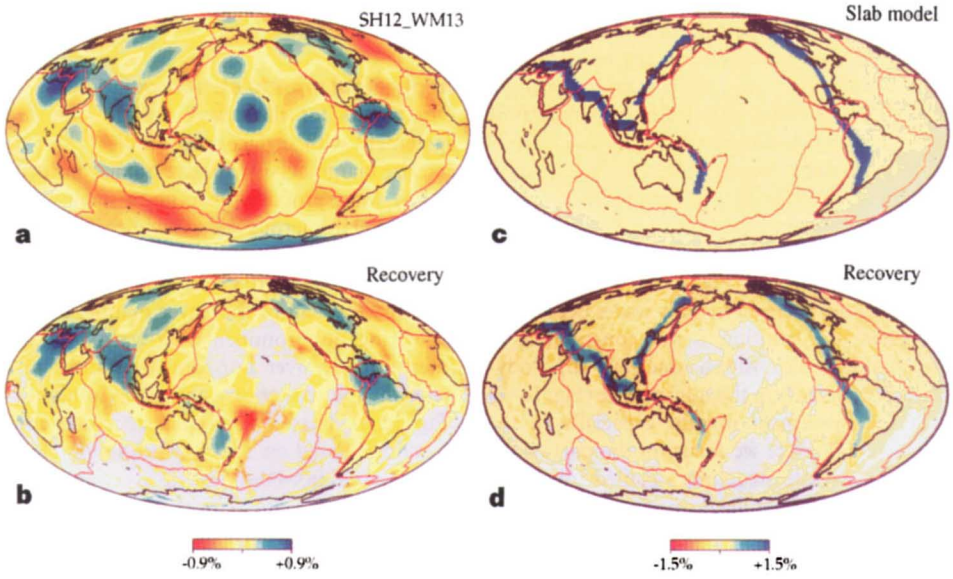

Figure 2 Resolution of long-wavelength (**a**, **b**) and short-wavelength (**c**, **d**) structure. We investigated the potential resolution of certain structural features in aspherical Earth models by inverting synthetic data calculated from assumed input models. We added gaussian noise to the synthetic data to simulate data errors and applied the same parameters (number of iterations, amount of regularization) as in the inversion of reported phase data. **a**, Lateral variation in shear-wave speed in the mid-mantle (at 1,300 km depth) according to *SH13_WM13* by Su and co-workers[33], and **b**, structure according to this model as it would have been imaged using the body-wave paths used in our study. Comparison of the input (**a**) and the recovery after inversion (**b**) demonstrates first, that our data coverage is sufficient, in particular in the Northern Hemisphere, to resolve large-scale structural features, and second, that there is significant agreement between the models if structures in *SH12_WM13* represent long-wavelength images of narrower structures (Figs 1d and 3). **c**, Artificial slab structure at 1,300 km depth with a peak anomaly of 3% (off-scale). The result of the inversion of the (noisy) synthetic data (**d**) demonstrates that narrow structure in the lower mantle can be resolved by our data, in particular in the Northern Hemisphere, and that the width of the anomaly may not be significantly overestimated. These tests also indicate that insufficient sampling by our body waves precludes the resolution of lower-mantle structures in large parts of the Southern Hemisphere. (Note that our colour coding intentionally de-emphasizes structure of near-zero amplitude. Inversion with random noise and the assessment of effects of, for instance, source mislocation and uneven data coverage suggest that structure with near-zero amplitude is not necessarily indicative of Earth's structure).

lower-mantle structure beneath the Americas is laterally coherent for depths up to approximately 1,700 km, but the slab signature vanishes at about 1,300 km depth beneath South America[22]. The deep anomaly connects to upper-mantle structures that are more fragmented as a result of Cenozoic tectonic activity in the eastern Pacific and Caribbean region. Beneath eastern Europe and Indonesia a fast anomaly can be traced from mid- to upper-mantle depths, but it is elsewhere only inferred between about 1,000 and at least 1,700 km in depth. The vertical dimension of both lineaments exceed the depth uncertainty in the images of about 300 km as determined by resolution tests with fabricated slab models (S.W. and R.D.v.d.H., manuscript in preparation). Outside these large-scale structures there is substantial scatter of smaller-scale heterogeneity, some of which may be real on the basis of correlation with independent results[22,42].

In the mid-mantle, slow anomalies appear isolated in map view. Their shape seems more equidimensional than the fast structures, but this is not well constrained owing to poor data coverage. A slow anomaly is visible from the Earth's surface to at least 2,000 km depth beneath the southwestern Pacific Ocean (Society islands) and from about 800 km depth to the CMB beneath southern and central Africa.

At about 1,700 km depth the character of heterogeneity begins to change: the linear structures (Fig. 1c, d) gradually disintegrate into smaller-scale anomalies that show less lateral continuity (Fig. 1e). In the lowermost mantle (2,300 km depth to the CMB), mantle structure is again dominated by long-wavelength features (Fig. 1f), but the general appearance of heterogeneity in this depth range is strikingly different from the linear structures at shallower depth (compare, for instance, Fig. 1d, f). There is general agreement between our results and independent studies of the region just above the CMB (see Wysession[43] and references therein), although there seem to be some differences between P- and S-wave speed that are not yet fully understood[42]. Our data do not satisfactorily resolve Southern Hemisphere structure but the global distribution of fast and slow anomalies is consistent with the heterogeneity pattern inferred from waveform data[33–35]. The images also reveal small-scale features that we think are real. For example, the short-wavelength variations at mid-latitudes in the western Pacific are in excellent agreement with anomalous core-phase (PKP) times (K. C. Creager, personal communication).

Are narrow structures in the mid-mantle real?

The inference that narrow features are prominent to at least 1,700 km depth in the Earth's mantle is perhaps surprising as spherical-harmonic representations of the Earth's interior shear structure indicate that the amplitude of structure in the mid-mantle is significantly lower than that in the upper and lowermost mantle structure, at least out to degree 16 (refs 33–35).

The length of the linear features exceeds by far the distance over which body waves propagate horizontally, indicating that a large number of data with coherent structural signal must contribute to the mapping of these structures. The narrow width of the lower-mantle lineaments is not an artefact owing to preferential sampling or the use of local basis functions for model parametrization (Fig. 2). With the body-wave paths used in the actual data inversion we computed travel times using the long-wavelength model by Su and co-workers[33]. We inverted these synthetic data and compared the

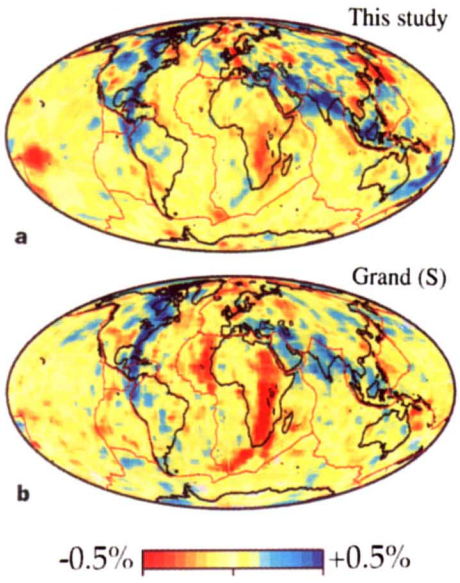

Figure 3 Africa-centred Mollweide projections of lateral variation in P- and S-wave speed at a depth of 1,350 km in different tomographic models of the Earth's mantle. The linear high-wave-speed anomalies revealed by inversion of our P-wave data (**a**) are in very good agreement with the results of S-wave inversions by Grand[22,42] (**b**). Grand's model is based on a careful analysis of direct and multiply reflected shear waves, and is continually being upgraded with more data. The wave-speed perturbations are plotted on the same scale, that is between ± 0.5% relative to the reference models used. For this comparison we choose to use a different projection than in Figs 1, 2 and 4 because mantle structure beneath the western Pacific is not yet well constrained in Grand's current models.

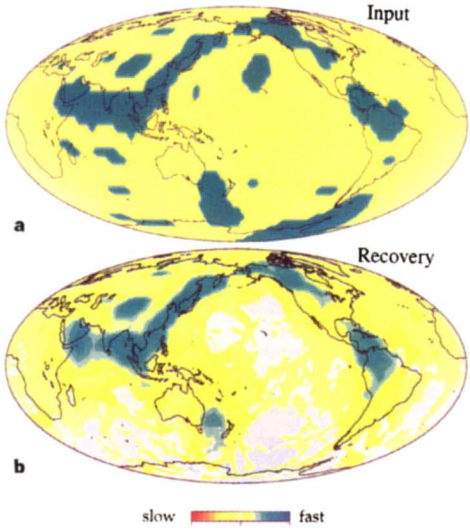

Figure 4 Illustration of the resolution of large-scale structures at depths between 1,800 and 2,000 km using a synthesized three-dimensional slab model[9] that is based on plate covergence in the past 180 Myr (refs 8, 44). This model is produced by 'simply' dropping spherical particles, called slablets, into the mantle beneath a convergence margin and does not account for ambient mantle flow or dynamical effects of the transition zone. The 'slabs' sink vertically across the upper/lower mantle interface, but at a reduced rate due to an increase in viscosity. We inverted synthetic data calculated from the three-dimensional slab model, shown in **a** at a depth of 1,900 km, and compared the recovered model (**b**) to the input model. We tested the resolution of such large-scale structures at ~1,900 km because this represents the depth interval where inversion of the actual data indicates a patchwork of smaller scale structure. The comparison suggests that: (1) upon the damped inversion there is a substantial loss of amplitude; (2) our data coverage is not sufficient to resolve structure in the Southern Hemisphere and the central Pacific; and (3) the circumpacific and south Asia anomalies would be well resolved, but smearing can produce structures with amplitudes less than ~20% of the peak values. Tests such as those illustrated here and in Figs 2 and 5 have several advantages over more standard 'chess-board' tests. In particular, one can investigate more directly whether the data used can resolve a hypothetical pattern of structural heterogeneity. This technique can help, for instance, to explore the class of seismic data required to verify certain aspects in numerical models.

output to the input model. The excellent model recovery indicates that our inversion technique does not bias towards short-wavelength anomalies in regions of dense sampling and implies that long-wavelength lower-mantle structures will be mapped accurately by our method if the data contain signal pertinent to such structures. This interpretation, if correct, suggests that spectral methods map similar structural features but may significantly overestimate their true width. Our resolution degrades in areas of poor sampling and substantial parts of the long-wavelength models cannot be tested against our results. Such tests thus help isolate structures for which a model comparison is meaningful.

Resolution tests also demonstrate that narrow structures can be resolved in most parts of the lower mantle and that their width can probably be inferred fairly accurately from Figs 1 and 3 (Fig. 2c, d). The increasing agreement between independent models further suggests that the linear anomalies are real. Once identified, the linear structures can be recognized in the long-wavelength models[33–35] (Fig. 2) and in images based on ISC data[37,38] but these models typically show high-amplitude structure in other regions as well, which complicates interpretation. Particularly exciting is the excellent correlation between the narrow structures in our P-wave maps and similar features in the S-wave model by Grand[22,42] (Fig. 3). There is good agreement also at depths other shown in Fig. 3 but differences exist in regions of poor data coverage in one or the other model, or both[42]. The spectacular correlation of structural detail in models deduced independently from different data and analysis procedures marks significant progress in global imaging.

Cold downwellings in the lower mantle

Figure 4a shows the lateral distribution (planform) of downwellings in the mid-mantle according to a synthesized three-dimensional slab model[9] based on plate convergence in the past 180 Myr (ref. 44) and a simple simulation of whole-mantle flow. Our data coverage is sufficient to map out the structure as predicted (Fig. 4), except for the region south of South America, which implies that many observed differences from the tomograms are meaningful.

The subduction model predicts significant slab structure in the mid-mantle beneath North America (subduction of the Farallon plate), southern Eurasia (Tethys ocean floor), the northwestern Pacific (Izanagi, Kula and Pacific plates) and Tonga (Pacific plate). The Farallon anomaly, the first lower-mantle structure associated with subduction[45] and discussed in more detail by Grand[22], is prominent in our images and appears to be continuous from the upper mantle to the CMB beneath central America (Fig. 5). In the upper 300 km, the narrow slab does not leave a signature in 2° × 2° blocks but shows up clearly when a smaller block size is used (H. Bijwaard *et al.*, personal communication). The subduction of former African lithosphere beneath Europe, often referred to as the Aegean slab, forms the western boundary of the Tethys anomaly in the mid-mantle beneath southern Eurasia (Fig. 6a). The Aegean slab seems to be continuous to approximately 1,500 km depth

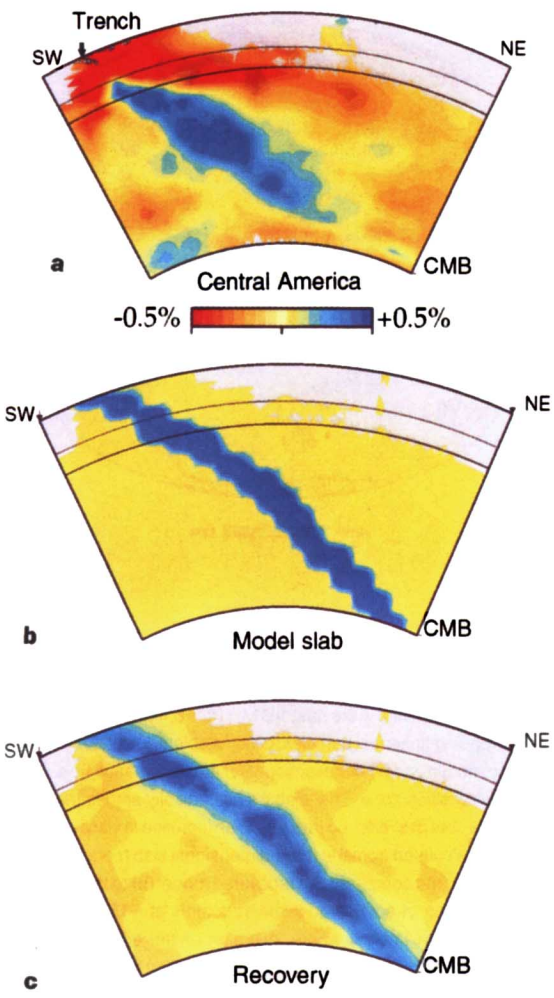

Figure 5 a, Vertical mantle section through our global P-wave model from the Earth's surface to the core-mantle boundary across the convergent margin in Central America (see Fig. 1a for cross-section location). This anomaly was one of the first lower-mantle structures interpreted as lithospheric slab in the lower mantle[45]; see Lay[13] for a recent review of this and other subduction-zone structures. The fast anomaly in the lower mantle has a peak value of almost 1% of the *ak135* reference model, but this value is not well constrained. As before, the poorly sampled mantle regions are masked. CMB, core-mantle boundary; NE and SW denote geographical orientation. The word 'trench' marks the location at the surface of the Middle America trench. Thin lines at constant depth depict the location of the 410 and 660 km discontinuities. The comparison of the input with a peak anomaly of 3% (**b**) and output (**c**) of test inversions with synthetic data (see Figs 2 and 4 for description) demonstrates that both the width and amplitude of the high-wave-speed anomaly beneath Central America are influenced by irregular sampling but that the slab is probably not much narrower than inferred from **a**. Results of studies at higher resolution (S.W. and R.D.v.d.H., manuscript in preparation) indicate continuity of the Farallon slab across the shallow mantle but that it is too narrow to be resolved in our current global inversion. Similar tests show that for Tonga the data can not discriminate between penetration to ~1,800 km or to a larger depth.

(Fig. 6b), which is in accord with a regional study[23]. The eastern edge of the Tethys structure is marked by subduction of the Indo-Australian plate beneath the Sunda arc[25].

The pattern of mantle flow beneath the northwestern Pacific remains enigmatic. On the basis of plate reconstructions for this region[8,9,44] one would expect a slab-related anomaly in the lower mantle that is as prominent as the Tethys and Farallon structures (Fig. 4). Even though our data coverage is sufficient to detect such a feature (Fig. 2c, d) we do not observe it in the depth range between approximately 700 and 1,400 km (Fig. 1c, d). This concurs with global models based on spherical harmonics: a circumpacific high is usually inferred, but in the top of the lower mantle beneath east Asia the fast anomaly is often either absent or significantly reduced in amplitude[33–35] (Fig. 2; H. Bolten and G. Masters, personal communication). At approximately 1,500 km depth a large-scale anomaly re-emerges that continues to the CMB (Fig. 1). Locally, narrow fast anomalies seem to pierce through the 'gap' in the uppermost lower mantle and connect to (and, indeed, cause) the pronounced high-wave-speed anomaly in the CMB region beneath eastern Asia (Fig. 6b).

Deep circulation in the Earth's mantle

Figures 1, 5 and 6 suggest that fast anomalies are continuous across the '660-km' discontinuity to at least 1,700 km depth beneath many convergent margins and that the long narrow structures in the mid-mantle are related to subduction of former oceanic lithosphere, with some slab segments probably sinking all the way to the CMB. Lower-mantle flow is required to explain these observations—the distance to the upper mantle is simply too large for them to be the result of conductive cooling alone—and must be causally related to upper-mantle flow unless the inferred spatial correlation of wavespeed anomalies is just coincidental. Flow across the seismic discontinuity offers the simplest explanation of the observed continuity of amplitude and geometry (for example, dip angle) of the anomalies. In particular, our results argue against worldwide mantle stratification by a flow-impeding interface at 660 km or stagnation of slab material in the lower mantle above 1,100 km (ref. 46). Penetrative convection—a hybrid flow model in which slab material flows back to the upper mantle after initial penetration into a chemically distinct lower mantle with slightly higher intrinsic density[10]—may explain our observations, in particular if the chemical boundary occurs at such a large depth that downwarping to the CMB is plausible or if large depressions of the boundary nucleate downwellings that control the planform of convection in the layer beneath them (mechanical coupling) and show up as fast anomalies. Either alternative is not easily distinguished from simple whole mantle flow on the basis of seismic imaging alone.

Local intermittence of flow into the lower mantle. Although inconsistent with worldwide stratification at 660 km depth the interplay of plate tectonic motions, radial increases in viscosity, and (perhaps) endothermic phase changes can locally distort mantle flow. Beneath the northwestern Pacific region, for example, some slabs deflect in the transition zone[20,21] whereas others penetrate to larger depth[18–20] (for example, Fig. 6b). Slab structure is here not well defined in the top of the lower mantle but re-emerges at larger depth (~1,500 km) and then continues to the

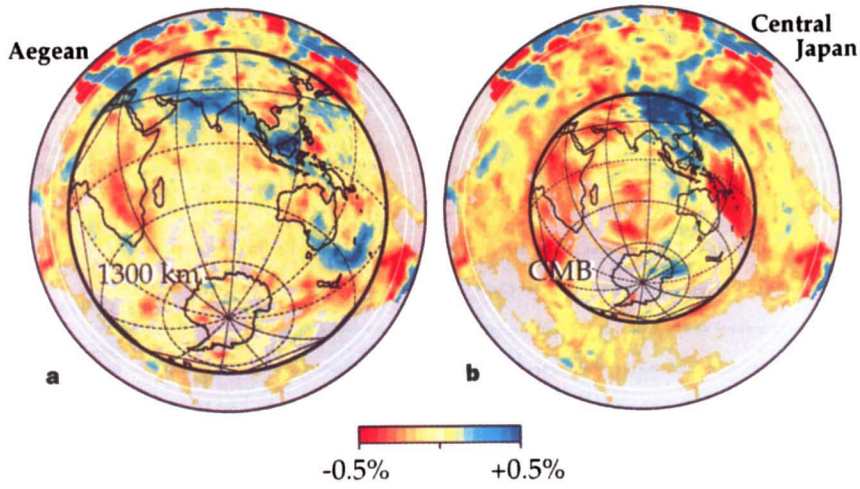

Figure 6 Mantle cross-sections along the great circle depicted in Fig. 1a to a depth of 1,300 km (**a**) and 2,750 km (**b**). In the centre of the vertical sections we plotted in map view the anomalies at the corresponding depth (that is 1,300 and 2,750 km) in an equal-area projection. The cross-section through the upper 1,300 km of the mantle demonstrates that the deep subduction of the African plate beneath eastern Europe[23] forms the western edge of the long linear structure that continues as an intermittent high-wave-speed anomaly beneath the southern margin of Asia and connects to the deep slab beneath Indonesia[25]. Beneath eastern Europe, the Aegean slab does not seem to have sunk deeper than about 1,500 km, in accord with the narrow width of the western part of the Mesozoic Tethys ocean. The depth to the leading edge of this slab is well constrained. Beneath central Japan we infer that the slab plunges into the lower mantle with an increased dip angle, which corroborates earlier studies based on residual sphere analyses[18] and travel-time inversion[19]. Beneath central Japan the narrow structure seems to be continuous to the core–mantle boundary, where it connects to the well studied seismic anomaly beneath southeastern Asia. This vertical continuity is only observed for rather narrow segments of the Japan slab; the results of extensive resolution tests suggest, however, that such detail can be resolved by the data used (for instance Fig. 2c, d). The map view at 1,300 km reveals that this deep subduction of the Pacific plate has not resulted in a linear structure large enough to be detected by our current study. This lack of structure is representative for the depth range between 800 and 1,400 km.

CMB. We argue that this structural complexity is in keeping with the complex tectonic evolution of the region and that mantle stratification is a local and transient[30–32] phenomenon with a characteristic timescale that is much shorter than that of mantle-wide overturn[47].

Lithospheric plates had been subducting along the eastern margin of continental Asia since at least 140 Myr ago (ref. 8) when Eocene (~45 Myr ago) plate reorganizations in the Pacific realm caused the separation of Japan from continental Asia and initiation of subduction beneath the Philippine Sea plate along the proto Izu Bonin and Mariana trenches. Post-Eocene clockwise migration of the newly formed arc system resulted in slab deflection in the transition zone beneath the Izu Bonin arc[47], which switched off the supply to the older downwelling in the lower mantle beneath the east Asian margin. The formation of the inferred 600 km or so slab window in the uppermost lower mantle during the past 40 Myr implies a minimum sinking rate of about 1.5 cm yr^{-1} in the lower mantle, which concurs with inferences from South America[22]. Trench migration may have caused local deflection of the Japan slab[47], but beneath central Japan subduction of the Pacific plate seems to have continued along a shallowly dipping conduit to a previously established downwelling anchored in the lower mantle[48] (Fig. 6b). Horizontal slabs are gravitationally unstable[49] and will eventually become entrained in lower-mantle flow through Rayleigh–Taylor instabilities; this process may produce narrow downwellings that may be hard to detect by seismic imaging.

Is there a lower-mantle transition zone? We infer from the images that flow in the shallow mantle connects, at least locally, to structural heterogeneity just above the CMB (Figs 5 and 6b), confirming previous suggestions of such a relationship[12,13,27,43,50], but the long narrow structures in the mid-mantle are strikingly different from the long-wavelength features just above the CMB (compare, for instance, Fig. 1d and f). This suggests that the downwellings that reach the CMB (Fig. 6b) lose the characteristic planar geometry across a transitional interval (approximately 1,800–2,300 km depth). A change in shape of the downwellings from sheet-like to more cylindrical is in accord with numerical flow simulations[51]. Comparison with other models also suggests that the change in character of heterogeneity is real. We remark that the inferred transition in heterogeneity coincides with a change in proportionality between P and S speed[52], indicated by the Poisson's ratio, which may indicate a compositional change[53]. There are several caveats. Although resolution tests demonstrate that the inferred breakdown of the linear structures is not a result of reduced sampling (Fig. 4) we realize that data coverage in the lowermost mantle is not satisfactory. Moreover, structural signal from heterogeneity in the deepest mantle may be lost from travel-time data owing to a mechanism known as wavefront healing[54]. At this stage we cannot exclude the possibility that the change in geometry of the anomalies is causally related to past changes in plate motion, without the need for a change in physical state. Conversely, it is exciting to realize that the detailed structures revealed by global imaging may now begin to constrain reconstructions of past plate motion.

It is obvious that several aspects of the tomographic model presented can—and will—be improved. There are important issues that require further study (uneven sampling, interpretation of deep structure, remaining differences with long-wavelength models), but there seems to be increasing consensus from seismology for deep convective circulation in the mantle. A concerted effort of seismic imaging, plate reconstruction, numerical flow modelling, and chemical mass-balancing is required to unravel reaming mysteries of the deep Earth and to explain the flow behaviour in a lower-mantle transition zone and the isotope record. The increasing similarity between flow patterns deduced from global seismic imaging and numerical flow simulation[55,56] (H.-P. Bunge and M. Richards, personal communication), and the fact that, for the first time, independent global wave-speed models begin to show excellent correlation of small-scale (<1,000 km) structure,[42] mark

important and exciting contributions towards understanding the dynamic and thermal evolution of our planet. □

Received 2 September 1996; accepted 11 March 1997.

1. Dziewonski, A. M., Hager, B. H. & O'Connell, R. J. Large-scale heterogeneities in the lower mantle. *J. Geophys. Res.* **82,** 239–255 (1977).
2. Dziewonski, A. M. Mapping the lower mantle: determination of lateral heterogeneity in P velocity up to degree and order 6. *J. Geophys. Res.* **89,** 5929–5952 (1984).
3. Carlson, R. W. Mechanisms of Earth differentiation: consequences for the chemical structure of the mantle. *Rev. Geophys.* **32,** 337–362 (1994).
4. Hofmann, A. Mantle geochemistry: the message from oceanic volcanism. *Nature* **385,** 219–229 (1997).
5. Hager, B. H., Clayton, R. W., Richards, M. A., Comer, R. P. & Dziewonski, A. M. Lower mantle heterogeneity, dynamic topography and the geoid. *Nature* **313,** 541–545 (1985).
6. Montagner, J.-P. Can seismology tell us anything about convection in the mantle? *Rev. Geophys.* **32,** 115–138 (1994).
7. Ritzwoller, M. H. & Lavely, E. M. Three-dimensional seismic model of the Earth's mantle. *Rev. Geophys.* **33,** 1–66 (1995).
8. Richards, M. A. & Engebretson, D. C. Large-scale mantle convection and the history of subduction. *Nature* **355,** 437–440 (1992).
9. Ricard, Y., Richards, M. A., Lithgow-Bertelloni, C. & Le Stunff, Y. A geodynamic model of mantle density heterogeneity. *J. Geophys. Res.* **98,** 21895–21909 (1993).
10. Silver, P. G., Carlson, R. W. & Olson, P. Deep slabs, geochemical heterogeneity, and the large-scale structure of mantle convection: investigations of an enduring paradox. *Rev. Earth Planet. Sci.* **16,** 477–541 (1988).
11. Jordan, T. H., Lerner-Lam, A. L. & Creager, K. C. in *Mantle Convection* (ed. Peltier, W. R.) 98–201 (Gordon & Breach Scientific, New York, 1989).
12. Davies, G. F. & Richards, M. A. Mantle convection. *J. Geol.* **100,** 151–206 (1992).
13. Lay, T. The fate of descending slabs. *Annu. Rev. Earth Planet. Sci.* **22,** 33–61 (1994).
14. Shearer, P. & Masters, G. Global mapping of topography on the 660-km discontinuity. *Nature* **355,** 791–796 (1992).
15. Ito. E. & Takahashi, E. Postspinel transformations in the system Mg_2SiO_4–Fe_2SiO_4 and some geophysical implications. *J. Geophys. Res.* **94,** 10637–10646 (1989).
16. Christensen, U. R. & Yuen, D. A. The interaction of subducting lithospheric slab with a chemical or phase boundary. *J. Geophys. Res.* **89,** 4389–4402 (1984).
17. Puster, P. & Jordan, T. H. How stratified is mantle convection? *J. Geophys. Res.* **102,** 7625–7646 (1997).
18. Creager, K. C. & Jordan, T. H. Slab penetration into the lower mantle below the Mariana and other island arcs of the northwest Pacific. *J. Geophys. Res.* **91,** 3573–3589 (1986).
19. Kamiya, S., Miyatake, T. & Hirahara, K. How deep can we see the high velocity anomalies beneath the Japan island arcs? *Geophys. Res. Lett.* **15,** 828–831 (1988).
20. Van der Hilst, R. D., Engdahl, E. R., Spakman, W. & Nolet, G. Tomographic imaging of subducted lithosphere below northwest Pacific island arcs. *Nature* **353,** 37–43 (1991).
21. Fukao, Y., Obayashi, M., Inoue, H. & Nenbai, M. Subducting slabs stagnant in the mantle transition zone. *J. Geophys. Res.* **97,** 4809–4822 (1992).
22. Grand, S. P. Mantle shear structure beneath the Americas and the surrounding oceans. *J. Geophys. Res.* **99,** 11591–11621 (1994).
23. Spakman, W., Van der Lee, S., Van der Hilst, R. D. Travel-time tomography of the European-Mediterranean mantle down to 1400 km. *Phys. Earth Planet. Inter.* **79,** 3–74 (1993).
24. Van der Hilst, R. D. Complex morphology of subducted lithosphere in the mantle beneath the Tonga trench. *Nature* **374,** 154–157 (1995).
25. Widiyantoro, S. & Van der Hilst, R. D. The slab of subducted lithosphere beneath the Sunda arc, Indonesia. *Science* **271,** 1566–1570 (1996).
26. King, S. D. The viscosity structure of the mantle. *Rev. Geophys. Suppl.* **33,** 11–17 (1995).
27. Loper, D. E. A simple model of whole mantle convection. *J. Geophys. Res.* **90,** 1809–1836 (1985).
28. Hedlin, M., Shearer, P. & Earle, P. S. Seismic evidence for small-scale heterogeneity throughout the Earth's mantle. *Nature* (in the press).
29. Krüger, F., Weber, M., Scherbaum, F. & Schlittenhardt, J. Evidence for normal and inhomogenous lowermost mantle and core-mantle boundary structure under the Arctic and northern Canada. *Geophys. J. Int.* **122,** 637–657 (1995).
30. Thoraval, C., Machetal, P. & Cazenave, A. Locally layered convection inferred from dynamic models of the Earth's mantle. *Nature* **375,** 777–780 (1995).
31. Machetel, P. & Weber, P. Intermittent layered convection in a model mantle with an endothermic phase change at 670 km. *Nature* **350,** 55–57 (1991).
32. Tackley, P. Mantle dynamics: Influence of the transition zone. *Rev. Geophys. Suppl.* **33,** 275–282 (1995).
33. Su, W.-J., Woodward, R. L. & Dziewonski, A. M. Degree 12 model of shear velocity heterogeneity in the mantle. *J.Geophys. Res.* **99,** 6945–6981 (1994).
34. Li, X.-D. & Romanowicz, B. Global mantle shear-velocity model developed using nonlinear asymptotic coupling theory. *J. Geophys. Res.* **101,** 22245–22272 (1996).
35. Masters, G., Johnson, S., Laske, G. & Bolton, H. A shear-velocity model of the mantle. *Phil. Trans. R. Soc. Lond. A* **354,** 1385–1411 (1996).
36. Masters, G., Jordan, T. H., Silver, P. G. & Gilbert, F. A spherical Earth structure from fundamental spheroidal-mode data. *Nature* **298,** 609–613 (1982).
37. Inoue, H., Fukao, Y., Tanabe, K. & Ogata, Y. Whole mantle P-wave travel-time tomography. *Phys. Earth Planet. Inter.* **59,** 294–328 (1990).
38. Vasco, D. W., Johnson, L. R., Pulliam, R. J. & Earle, P. S. Robust inversion of IASP91 travel time residuals for mantle P and S velocity structure. *J. Geophys. Res.* **99,** 13727–13755 (1994).
39. Engdahl, E. R., Van der Hilst, R. D. & Buland, R. P. Global teleseismic earthquake relocation with improved travel times and procedures for depth determination. *Bull. Seismol. Soc. Am.* (submitted).
40. Kennett, B. L. N., Engdahl, E. R. & Buland, R. Constraints on seismic velocities in the Earth from traveltimes. *Geophys. J. Int.* **122,** 108–124 (1995).
41. Nolet, G. Solving or resolving inadequate and noisy tomographic systems. *J. Comput. Phys.* **61,** 463–482 (1985).
42. Grand, S. P., Van der Hilst, R. D. & Widiyantoro, S. Global seismic tomography: a snapshot of convection in the earth. *Geol. Soc. Am. Today* (in the press).
43. Wysession, M. E. Continents of the core. *Nature* **381,** 373–374 (1996).
44. Lithgow-Bertelloni, C., Richards, M. A., Ricard, Y., O'Connell, R. J. & Engebretson, D. C. Toroidal-poloidal partitioning of plate motions since 120 Ma. *Geophys. Res. Lett.* **20,** 375–378 (1993).
45. Jordan, T. H. & Lynn, W. S. A velocity anomaly in the lower mantle. *J. Geophys. Res.* **79,** 2679–2685 (1974).
46. Wen, L. & Anderson, D. L. The fate of slabs inferred from seismic tomography and 130 million years of subduction. *Earth Planet. Sci. Lett.* **133,** 185–198 (1995).
47. Van der Hilst, R. D. & Seno, T. Effects of relative plate motion on the deep structure and penetration depth of slabs below the Izu-Bonin and Mariana island arcs. *Earth Planet. Sci. Lett.* **120,** 375–407 (1993).
48. Griffiths, R. W., Hackney, R. & Van der Hilst, R. D. A laboratory investigation of trench migration and the fate of subducted slabs. *Earth Planet. Sci. Lett.* **133,** 1–17 (1995).
49. Christensen, U. R. The influence of trench migration on slab penetration into the lower mantle. *Earth Planet. Sci. Lett.* **140,** 27–39 (1996).
50. Kendall, J.-M. & Silver, P. G. Constraints from seismic anisotropy on the nature of the lowermost mantle. *Nature* **381,** 409–412 (1996).
51. Bercovici, D., Schubert, G. & Glatzmaier, G. 3-dimensional spherical-models of convection in the Earth's mantle. *Science* **244,** 950–955 (1989).
52. Bolton, H. & Masters, G. A region of anomolous $d \ln V_s / d \ln V_p$ in the deep mantle. (abstr.) *Eos* **77,** F6g7 (1996).
53. Loper, D. & Lay, T. The core-mantle boundary region. *J. Geophys. Res.* **100,** 6397–6420 (1995).
54. Nolet, G. & Moser, T.-J. Teleseismic delay times in a 3-dimensional Earth and a new look at the S-discrepancy. *Geophys. J. Int.* **114,** 185–195 (1993).
55. Puster, P., Hager, B. H. & Jordan, T. H. Mantle convection experiments with evolving plates. *Geophys. Res. Lett.* **22,** 2223–2226 (1995).
56. Bunge, H.-P., Richards, M. A. & Baumgardner, J. R. The effect of viscosity stratification on mantle convection. *Nature* **379,** 436–438 (1996).

Acknowledgements. We thank B. Kennett and J. Braun for providing graphics software; S. Grand, C. Lithgow-Bertelloni and W.-J. Su for access to their models; T. Jordan, B. Hager, S. Grand and C. Froidevaux for discussions; and G. Masters for a review. This work was supported in part by the US National Science Foundation.

Correspondence and requests for materials should be addressed to R.D.v.d.H. (e-mail: hilst@mit.edu).